Effect of Molecular Parameters on the Shrinkage of Injection-Molded Polypropylene

MITSUYOSHI FUJIYAMA, *Research and Development Division, Tokuyama Soda Co., Ltd.*, and SHUKICHI KIMURA, *Plastic Division, Tokuyama Soda Co., Ltd., Tokuyama-shi, Yamaguchi-ken, Japan*

Synopsis

The effect of some molecular parameters on the mold shrinkage, annealing shrinkage, and melting shrinkage of injection-molded polypropylene was studied. The mold shrinkage in the machine direction (MD) became higher as the melt flow index (MFI) became lower and the molecular weight distribution became broader. On the other hand, the mold shrinkage in the transverse direction (TD) showed a similar value (about 1.6%), regardless of the kind of resin, except for a glass fiber-reinforced polypropylene which showed a very low value. The annealing shrinkage and melting shrinkage showed similar tendencies as the mold shrinkage. The mold shrinkage and annealing shrinkage in the MD were in linear relationships with the thickness of the skin layer having positive slopes; the melting shrinkage in the MD was in a downward-curved relationship with the thickness of the skin layer having a positive slope, respectively, regardless of the cylinder temperature and the kind of resin.

INTRODUCTION

The mold shrinkage is an important property since in injection molding the precise value of the mold shrinkage of the resin is needed for the design of a mold, and, once the dimension of the mold is decided, the mold shrinkage pertains directly to the dimensional precision of molded articles.

Since the dimensions of injection-molded articles change with time, dimensional stability is also an important property. The shrinkage of the processed articles of crystalline polymers is caused mainly by the strain relaxation of expanded molecular chains in the amorphous region; thus, the concept of the time–temperature reduction principle,[1] which is often used when treating the viscoelasticity of an amorphous polymer, is applicable to the shrinkage. If this concept is applied, the annealing shrinkage at higher temperatures corresponds to the shrinkage at room temperature at longer time and hence is regarded as accelerated shrinkage at room temperature. Furthermore, the annealing shrinkage at high temperature is directly related to the dimensional stability of the molded article when it is used at a high temperature (for example, sterilization in boiling water).

Since the mold shrinkage and annealing shrinkage of an injection-molded article are closely related to its dimensional precision and dimensional stability it is not an exaggeration to say that they must be of great importance when we evaluate and/or design the quality of injection-molded articles.

The effect of injection molding conditions on the mold shrinkage and annealing shrinkage of injection-molded polypropylene (PP) was studied in the previous paper.[2] The mold shrinkage increased as the cylinder temperature and injection

pressure decreased and as the mold temperature increased, and was almost independent of the injection speed. On the other hand, the annealing shrinkage increased as the cylinder temperature decreased, and was almost independent of the injection pressure, mold temperature and injection speed. The mold and annealing shrinkages were in a linear relationship with the thickness of the skin layer having positive slopes, regardless of the cylinder temperature.

A few studies[3,4] have been done on the effect of molecular parameters on the shrinkages of injection-molded PP. Takashima et al.[3] studied the effect of melt flow index (MFI) on the mold shrinkage and annealing shrinkage of injection-molded PP, and found that the mold shrinkage was independent of the MFI in both MD and TD, while the annealing shrinkage increased in the MD and decreased slightly in the TD with reducing MFI. Keskkula et al.[4] measured the annealing shrinkages of injection-molded PPs near their melting points and found that they increased rapidly with reducing MFI.

This work deals with the effect of some molecular parameters such a MFI, molecular weight distribution, tacticity, random and block copolymerization with ethylene, and glass fiber-filling on the mold shrinkage, annealing shrinkage, melting shrinkage, and their anisotropies of injection-molded PP. From the view point of the orientation effect of molecular chains, experimental results were discussed in terms of the thickness of the skin layer.

TABLE I
Sample Properties

Sample	MFI, dg/min	$\eta_0/[|\eta^*|(\omega = 1 \text{ sec}^{-1})]$	Crystalliza- tion time, sec	Ethylene content, wt-%	Remarks
A	0.55	3.77	48	—	straight PP
B	0.66	4.61	41	—	straight PP
C	0.67	2.19	36	—	straight PP
D	1.2	3.80	30	—	straight PP
E	1.3	2.69	41	—	straight PP
F	1.5	3.01	35	—	straight PP
G	1.6	3.90	37	—	straight PP
H	3.9	3.13	30	—	straight PP
I	4.5	2.59	29	—	straight PP
J	5.9	3.16	35	—	straight PP
K	8.2	2.74	30	—	straight PP
L	8.4	2.79	30	—	straight PP
M	14.4	2.59	32	—	straight PP
N	2.2	1.54	64	—	low-tactic PP heptane extract = 23 wt-%
O	4.2	2.65	193	1.8	random copolymer with ethylene
P	9.6	2.80	50	0.5	random copolymer with ethylene
Q	1.9	3.48	30	12.0	block copolymer with ethylene
R	2.3	21.09	34	14.6	block copolymer with ethylene
S	2.1	—	17	—	FRPP glass fiber content 20 wt-%

EXPERIMENTAL

Materials

Materials used are shown in Table I: samples A to N are straight PPs; N is a low-tacticity PP with a heptane extract of 23 wt-%; O and P are random copolymers with ethylene; Q and R are block copolymers with ethylene; and S is a glass fiber-reinforced PP (FRPP) with a glass fiber content of 20 wt-%. The MFI was measured with a 2160-g load at 230°C according to ASTM D1238-62T. The ratio of the zero-shear viscosity η_0 to the absolute value of the complex viscosity at angular frequency of 1 sec^{-1}, $|\eta^*|(\omega = 1 \text{ sec}^{-1})$, namely, $\eta_0/[|\eta^*|(\omega = 1 \text{ sec}^{-1})]$, was used as a measure of the molecular weight distribution. η_0 and $|\eta^*|(\omega = 1 \text{ sec}^{-1})$ were measured at 190°C with a concentric cylinder rheometer (Rheometer Almighty, manufactured by Iwamoto Seisakusho Co., Ltd.).

In general, since at the region where angular frequency ω and shear rate $\dot{\gamma}$ are low, $|\eta^*|(\omega)$ and $\eta(\dot{\gamma})$ are equivalent functions,[5] and the reduction of $\eta(\dot{\gamma})$ with an increase in $\dot{\gamma}$ (non-Newtonian) becomes higher as the molecular weight distribution becomes broader,[6] $\eta_0/|\eta^*|(\omega = 1 \text{ sec}^{-1})$ becomes higher as the molecular weight distribution becomes broader. The crystallization time was measured on a specimen 0.3 mm thick with a differential scanning calorimeter. After the

TABLE II
Cylinder Temperatures[a]

Cylinder temp., °C	FZ, °C	CZ, °C	MZ, °C	AD, °C
190	180	180	190	180
220	180	200	220	200
250	180	230	250	230
280	180	260	280	260

[a] FZ = feed zone; CZ = compression zone; MZ = metering zone; AD = adaptor.

TABLE III
Injection Pressure at Different Cylinder Temperatures

Sample	Injection pressure, kg/cm^2			
	190°C	220°C	250°C	280°C
A	—	500	—	400
B	—	450	—	370
C	—	500	—	—
D	—	400	—	350
E	—	400	—	350
F	—	400	—	350
G	450	400	350	350
H	—	400	—	350
I	—	400	—	350
J	—	400	—	350
K	400	400	350	300
L	—	400	—	300
M	—	400	—	300
N	—	400	—	—
O	—	400	—	350
P	—	400	—	300
Q	—	400	—	350
R	—	400	—	350
S	400	400	350	350

specimen was annealed at 230°C for 10 min, the temperature was suddenly reduced to 110°C. The crystallization time equalled the period from the temperature decrease to 110°C to the peak maximum shown on an exothermic curve. The temperature was decreased to 110°C in about 62 sec for all samples.

Molding

To obtain specimens of uniform anisotropy, square plates were injection molded by use of a mold with a film gate (Fig. 1). Injection molding was carried out with a Toshiba IS 200A-Type 20-ounce reciprocating-screw injection molding machine. When the mold shown in Figure 1 was used, the flow of the resin in it was uniform.[7] Injection molding conditions were as follows: injection time, 8 sec; adjusting time, 10 sec; cooling time, 30 sec; mold temperature, 40°C; revolution speed of screw, 34 rpm; stroke measuring, 40 mm; injection speed, E-0 (max); cylinder temperature, see Table II; injection pressure, see Table III.

The cylinder temperature was measured at the metering zone (MZ). Although it was preferable to maintain the injection pressure constant when the resin and/or the cylinder temperature were changed, it was necessary to change it in order to shut out the short-shot and/or flash. However, since the change of the injection pressure was small and the injection pressure was kept constant for the resins with similar MFI, there was no problem in changing the injection pressure.

Shrinkage Measurements

The molded specimens were left in a constant-temperature (23°C) room for at least 48 hr after they were injection molded; the dimensions (L) were measured with a micrometer, and the mold shrinkage was calculated by eq. (1):

$$\text{mold shrinkage (\%)} = \frac{L_0 - L}{L_0} \times 100 \qquad (1)$$

where L_0 is the dimension of the mold cavity.

The injection-molded specimens were annealed at a fixed temperature for a fixed time in an oven and left at the constant temperature of 23°C for at least 24 hr. The dimensions L_a were measured with a micrometer, and the annealing shrinkage was calculated by eq. (2):
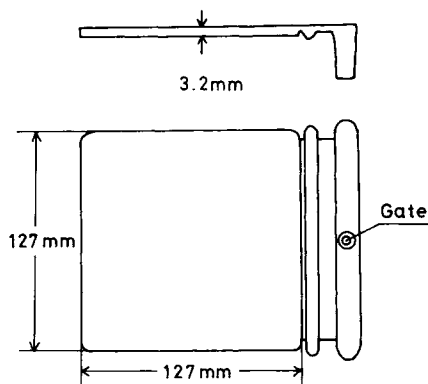

Fig. 1. Shape of mold cavity.

$$\text{annealing shrinkage (\%)} = \frac{L - L_a}{L} \times 100 \tag{2}$$

where L is the dimension before annealing. Annealing was carried out at 100°C for 36 hr, at 134°C for 20 hr, and at 155°C for 2 hr.

The injection-molded specimens were melted in a 190°C oven and shrunk freely for 10 min. They were then solidified at room temperature, the dimensions L_m were measured, and the melting shrinkage was calculated by eq. (3):

$$\text{melting shrinkage (\%)} = \frac{L - L_m}{L} \times 100 \tag{3}$$

The melting shrinkage was measured only in the MD.

The anisotropies of the mold and annealing shrinkages were expressed by the shrinkages in the MD minus those in the TD.

RESULTS AND DISCUSSION

Mold Shrinkage

Since the shrinkage of the injection-molded square plate differed from place to place, for convenience we used the shrinkage along the center line in both the MD and TD.

The variation of the mold shrinkage of the square plate molded at 220°C with the MFI is shown in Figure 2. The open and closed circles are for the MD and TD, respectively. The mold shrinkage in the MD increases with decrease in MFI. Compared on the same MFI level, the mold shrinkage becomes higher as the molecular weight distribution becomes broader (B > C, D > E, G > F, and H > I). A block copolymer with ethylene, Q shows a higher mold shrinkage than the straight PP with similar MFI as Q; and a low-tactic PP, N shows a lower mold shrinkage than the straight PP with similar MFI as N. Since sample N has a very narrow molecular weight distribution in addition to low tacticity, the molecular weight distribution may play an important role. Sample S, an FRPP, shows a very low mold shrinkage. It is assumed that glass fibers restrict shrinkage.
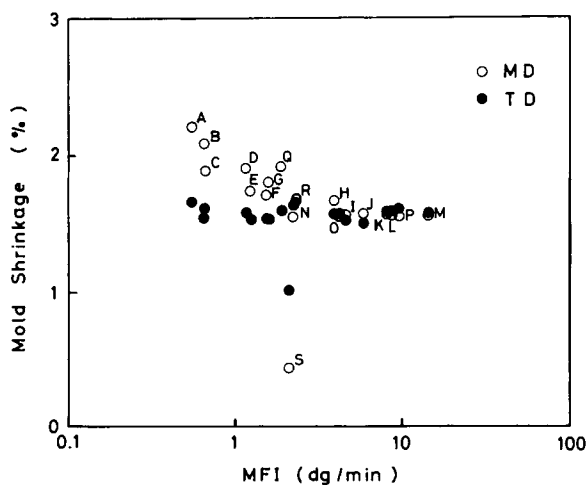

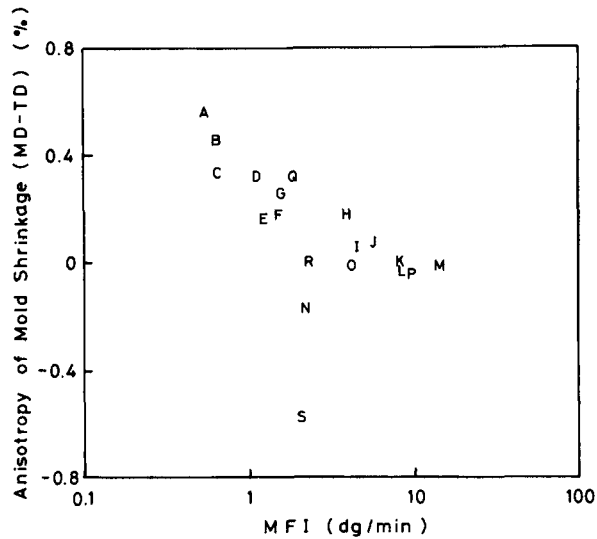Fig. 2. Variations in mold shrinkage of square plates molded at 220°C with MFI.

Fig. 3. Variation in anisotropy of the mold shrinkage (MD − TD) of square plates molded at 220°C with MFI.

Except for sample S, the mold shrinkage in the TD shows a similar value (about 1.6%) for all samples.   Mold shrinkage is governed mainly by orientation and crystallization effects.   Mold shrinkage in the TD is scarcely affected by the orientation effect; it is assumed that the crystallization effect upon mold shrinkage, even for the random and block copolymers with ethylene and low-tactic PP, does not differ much from that for the straight PPs.   Although the crystallization times measured at 110°C of the random copolymers with ethylene and the low-tactic PP are longer than those of the straight PPs (Table I), the mold shrinkages in the TD of these PPs does not differ from those of the straight PPs. It is assumed that since the polymer melt is quenched to a much lower temperature than 110°C in injection molding, the crystallization characteristic measured at the low degree of supercooling does not affect the mold shrinkage in the TD.
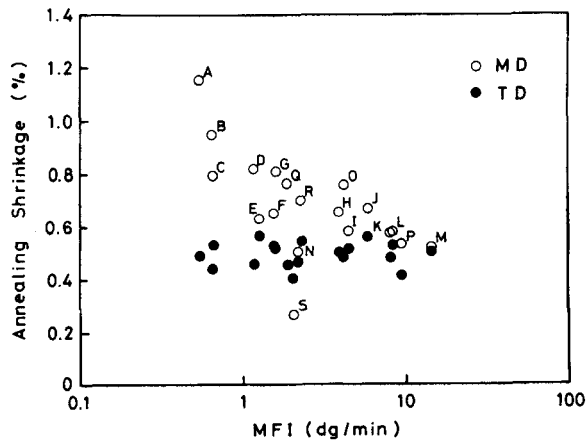

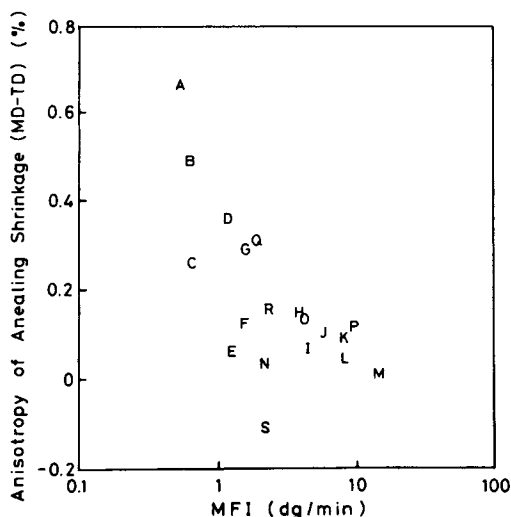Fig. 4. Variations in the 134°C annealing shrinkage of square plates molded at 220°C with MFI.

Fig. 5. Variations in the anisotropy of the 134°C annealing shrinkage of square plates molded at 220° with MFI.

The variation in anisotropy of the mold shrinkage (MD − TD) with MFI is shown in Figure 3. The orientation effect on mold shrinkage can be evaluated if MD-TD is calculated, since the crystalization effect acts equally on both the MD and TD. There is a tendency for the anisotropy of the mold shrinkage to decrease with increasing MFI, and it becomes lower as the molecular weight distribution becomes narrower. Sample N, a low-tactic PP, shows a very low anisotropy. The fact that the mold shrinkage in the TD of sample N does not differ from those of other PPs suggests that the low anisotropy of sample N is not due to its low crystallization characteristic but to its very narrow molecular weight distribution.

Although the mold shrinkages and their anisotropies were also measured for the specimens molded at 280°C, they showed similar tendencies as those molded at 220°C, except that the absolute values of the mold shrinkages in the MD and their anisotropies were lower than those molded at 220°C. The fact that the absolute values of the mold shrinkages in the MD (and their anisotropies of the specimens molded at 280°C) are lower than those molded at 220°C may be due to thinner skin layers.

Annealing Shrinkage

The variations in the 134°C annealing shrinkage of the square plate molded at 220°C and its anisotropy with the MFI are shown in Figures 4 and 5, respectively. Although the 100° and 155°C annealing shrinkages were also measured, they showed similar tendencies as the 134°C annealing shrinkage, with the exception that the absolute values of the annealing shrinkage in the MD and its anisotropy were lower and higher for the former and the latter, respectively. Further, although the annealing shrinkages and their anisotropies at various temperatures were measured for the specimens molded at 280°C, they showed similar tendencies as those molded at 220°C, except that the absolute values of the annealing shrinkages in the MD and their anisotropies were lower than those molded at 220°C. These annealing shrinkages and their anisotropies show nearly
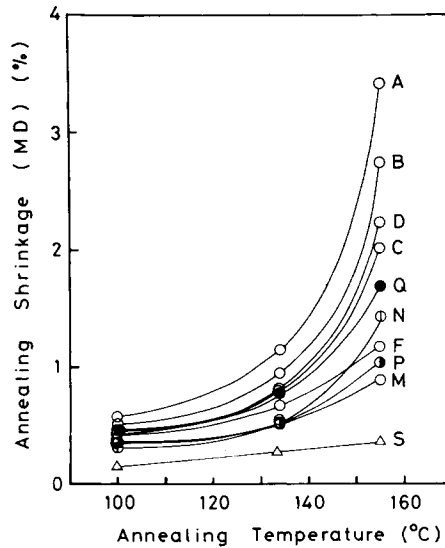
Fig. 6. Variations in the annealing shrinkage in the MD of square plates molded at 220°C with annealing temperature.
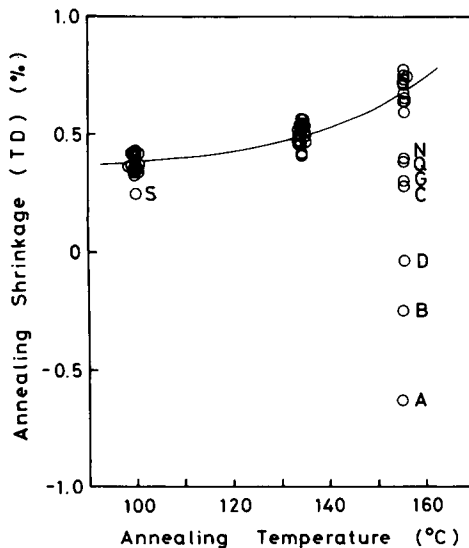

Fig. 7. Variations in the annealing shrinkage in the TD of square plates molded at 220°C with annealing temperature.

similar tendencies as the mold shrinkage and their anisotropies, respectively. Namely, the annealing shrinkage in the MD and its anisotropy become higher as MFI decreases and the molecular weight distribution broadens.

The variations in annealing shrinkages in the MD and TD of the specimens molded at 220°C with annealing temperature are shown in Figures 6 and 7, respectively. Although the annealing shrinkages in the MD of all samples are not shown, the sample with high annealing shrinkage in the MD generally shows the largest variation of the annealing shrinkage in the MD with annealing temperature. But the random copolymers with ethylene (samples O and P) and low-

tactic PP (sample N) show higher annealing shrinkages than the straight PP with similar MFI as those at a high annealing temperature, while they show lower annealing shrinkages than the straight PP at low annealing temperatures. This fact is due to their low melting points.

The annealing shrinkage in the TD slightly increases with increase in annealing temperature. While the 100° and 134°C annealing shrinkages in the TD are nearly the same, regardless of the kind of resin, the 155°C annealing shrinkage shows lower annealing shrinkages in the TD than the group of samples with lower annealing shrinkages in the MD. This tendency becomes more noticeable as the annealing shrinkage in the MD becomes higher. This is probable because, in high-temperature annealing such as at 155°C, the samples with high annealing shrinkage in the MD shrink very much in the MD and expand in the TD, and thickness varies according to the amount of shrinkage.

Melting Shrinkage

In injection molding, the molten resin flows into a cavity at high shear rate and possesses not only viscous deformation (flow) but also elastic deformation. A part of the elastic deformation, which does not relax, remains in the molded article as a frozen-in strain in the form of molecular chain orientation. If the molded article is remelted, the frozen-in strain must fully relax, and from the amount of the shrinkage which then occurs we can evaluate, to some extent, the amount of the frozen-in strain and the amount of the elastic deformation.

The melting shrinkage in the MD of the square plates molded at 220°C is shown in Figure 8. The melting shrinkage in the MD becomes higher as the MFI becomes lower and the molecular weight distribution becomes broader. It is assumed that the higher the molecular weight and the broader the molecular weight distribution, the larger the elastic deformation the polymer melt undergoes in injection molding and hence the larger the frozen-in strain in the molded
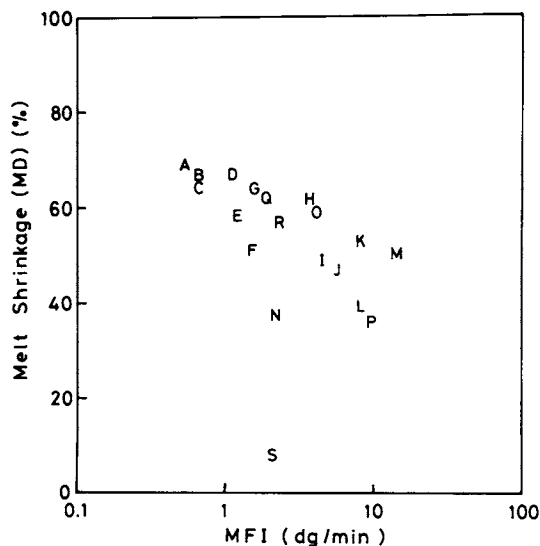

Fig. 8. Variations in the melting shrinkage in the MD of square plates molded at 220°C with MFI.

Fig. 9. Example of skin/core morphology. Sample A molded at 220°C.
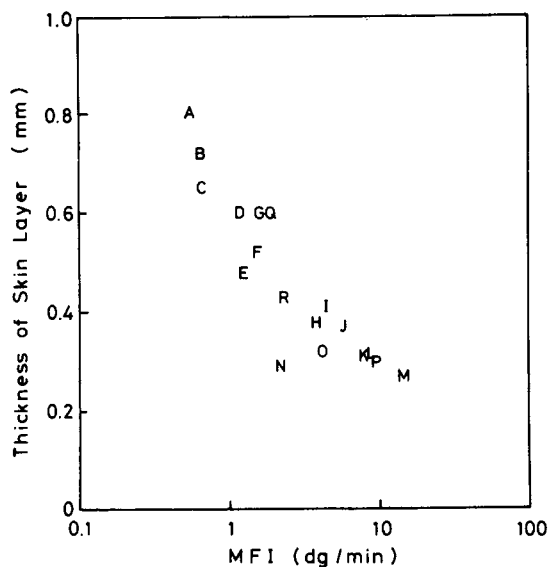

Fig. 10. Variations in thickness of skin layer of square plates molded at 220°C with MFI.

article. The melting shrinkage amounts to 70% in the highest case, which means
that the injection-molded article shrinks to one quarter of its original length by
melting. In such a case, it may be better to say that the molten resin is forcibly
packed into the cavity by elastic deformation rather than by flow.

The melting shrinkages of the square plates molded at 280°C showed a similar
tendency as those molded at 220°C, except that the absolute values of the former
were lower than those of the latter.

Thickness of Skin Layer

An injection-molded PP shows a clear skin/core morphology when it is ob-
served by a polarized microscope.[2,8] An example of the skin/core morphology
is shown in Figure 9. The variation in thickness of the skin layer at the center
area of the square plate with the MFI is shown in Figure 10. The thickness of
the skin layer increases with decrease in MFI, and, compared on the same MFI
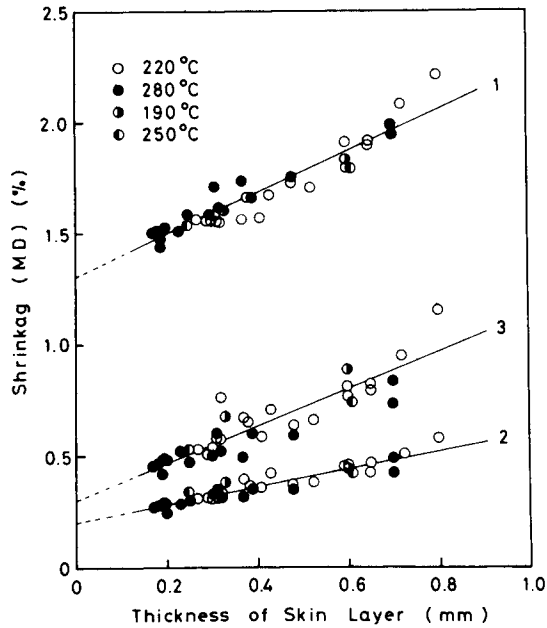level, becomes higher as the molecular weight distribution becomes broader.

Fig. 11. Relationship between thickness of skin layer and (1) mold shrinkage in the MD, (2) 100°C annealing shrinkage in the MD, and (3) 134°C annealing shrinkage in the MD. Key to cylinder temperatures at which samples were molded is given in upper left-hand corner of figure.
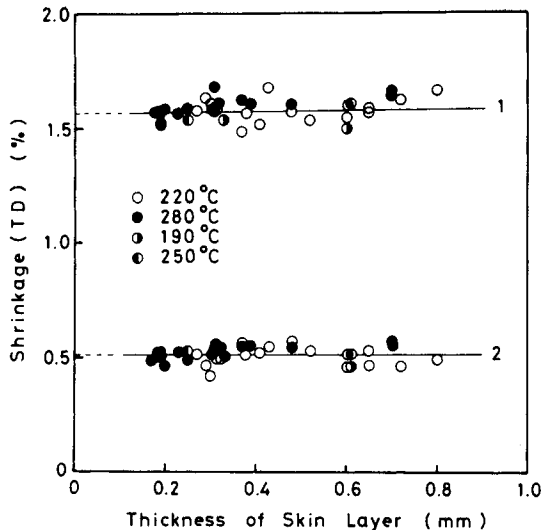

Fig. 12. Relationship between thickness of skin layer and (1) mold shrinkage in the TD and (2) 134°C annealing shrinkage in the TD. Key to cylinder temperatures at which samples were molded is shown in middle part of figure.

The thicknesses of the skin layers of the square plates molded at 280°C showed a similar tendency as those molded at 220°C, except that the absolute values of the former were lower than those of the latter. The variation in thickness of the skin layer with the MFI shows a similar tendency as the variations of the mold, annealing, and melting shrinkages with the MFI.

Relation Between Shrinkage and Thickness of Skin Layer

The relationships between the mold and annealing shrinkage in the MD and TD and the thickness of the skin layer are shown in Figures 11 and 12, respectively. There are linear relationships with positive slopes between the various shrinkages in the MD and the thickness of the skin layer. There are linear relationships between the various shrinkages in the MD and the thickness of the skin layer when the specimens are injection molded with the same resin at varying molding conditions (cylinder temperature).[2] There are also linear relationships between the various shrinkages in the MD and the thickness of the skin layer when the specimens are injection molded with varying resin at constant molding conditions (Fig. 11). From these facts, it can be said that the change of the shrinkages in the MD, which occurs when the specimens are injection molded with different kinds of resins and different molding conditions (cylinder temperature), is governed by the thickness of the skin layer.

In general, the factors which govern mold shrinkage of crystalline polymers[2] are (1) volumetric shrinkage by crystallization, (2) thermal shrinkage which originates in the expansion coefficient, (3) orientation of molecular chains, and (4) elastic recovery of the polymer melt. Of these factors, (1), (2), and (3) act in the direction of increasing mold shrinkage, and (4) acts in the direction of decreasing mold shrinkage. Since the orientation of molecular chains is condensed in the skin layer, the thickness of the skin layer can be used as a measure of the molecular chain orientation. Since the mold shrinkage varies from 1.5% to 2.2% (Fig. 11) when the thickness of the skin layer changes from 0.2 to 0.8 mm, the molecular chain orientation effect, factor (3) mentioned above, plays a considerable role in mold shrinkage. When the thickness of the skin layer is extrapolated to zero, there still remains a 1.3% mold shrinkage. The annealing shrinkage in the MD becomes 0.2%–0.3%, and this is governed mainly by the molecular chain orientation effect.
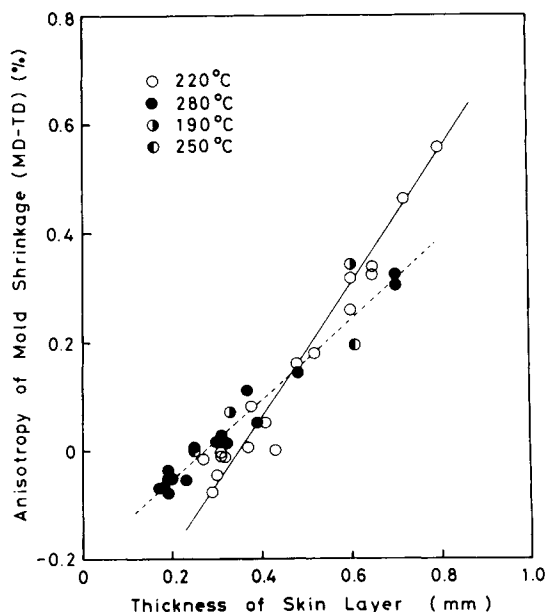

Fig. 13. Relationship between anisotropy of mold shrinkage (MD − TD) and thickness of the skin layer. Key to cylinder temperatures at which samples were molded is shown in upper part of figure.
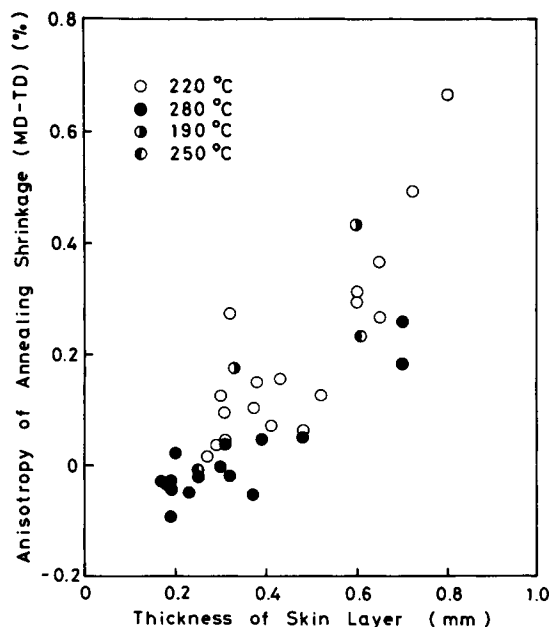
Fig. 14. Relationship between anisotropy of 134°C annealing shrinkage (MD − TD) and thickness of the skin layer. Key to cylinder temperatures at which samples were molded is shown in upper part of figure.

At the same time, the mold and annealing shrinkages in the TD are constant (mold shrinkage, 1.6%; 134°C annealing shrinkage, 0.5%) and independent of the thickness of the skin layer, which means that shrinkage in TD is not affected by the molecular chain orientation.

The relationships between the anisotropies of the mold shrinkage and 134°C annealing shrinkage (MD − TD) and the thickness of the skin layer are shown in Figures 13 and 14, respectively. The reason why MD − TD is adopted as a measure of shrinkage anisotropy is that the effect of molecular chain orientation can be estimated if MD − TD is taken since the factors, other than molecular chain orientation, act similarly on the shrinkage in both the MD and TD.

The relationship between the anisotropy of the mold shrinkage and the thickness of the skin layer is linear, and hence it is assumed that the molecular chain orientation is condensed in the skin layer. This fact is supported by the structure analysis of the skin and core layers in the previous paper.[9] The 220°C- and 280°C-molded specimens are on different lines, which is probably due to the difference in the quality of the skin layer. The fact that the slope of the line for 220°C-molded specimens is steeper than that for the 280°C-molded specimens suggests that the skin layers of the 220°C-molded specimens have a higher degree of molecular chain orientation than those of the 280°C-molded specimens. Further, the anisotropy of the mold shrinkage does not become zero at zero thickness of the skin layer, but becomes zero at 0.3-mm thickness of the skin layer, which is assumed to be due to the anisotropy of the injection pressure (the pressure in the MD is higher than that in the TD) and the expansion in the TD and thickness direction by the amount of shrinkage in the MD.
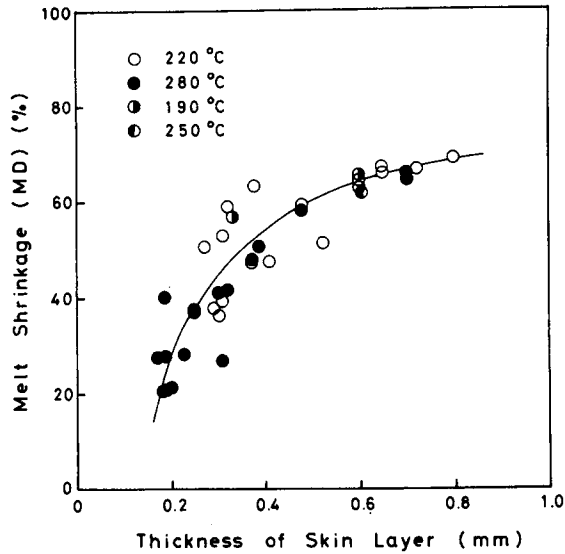
Fig. 15. Relationship between melting shrinkage in the MD and thickness of the skin layer. Key to cylinder temperatures at which samples were molded is shown in upper part of figure.

There is also a positive correlation between the anisotropy of the 134°C annealing shrinkage and the thickness of the skin layer, though it is not so close as in the case of the anisotropy of the mold shrinkage. In this correlation, the resin with a narrower molecular weight distribution shows a lower anisotropy than the resin with a broader molecular weight distribution for the thickness of the skin layer.

Finally, the relation between the melting shrinkage in the MD and the thickness of the skin layer is shown in Figure 15. There is a positive correlation, and it is assumed that the greater part of the frozen-in strain is condensed in the skin layer.
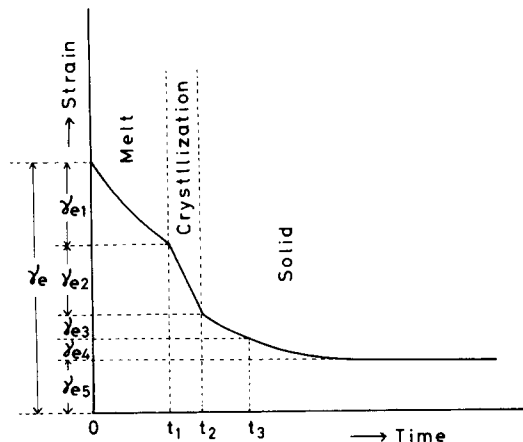

Fig. 16. Schematic diagram for variation of recoverable shear strain with time. Molten resin is injected into the mold at $t = 0$. Crystallization begins at $t = t_1$ and terminates at $t = t_2$.

DISCUSSION

If the recoverable shear strain which a molten resin possesses just after it is injected into a cavity on injection molding is γ_e, (Fig. 16), it is assumed that a portion of it, γ_{e1}, relaxes during the molten state before solidification by crystallization ($0 < t < t_1$); a portion, γ_{e2}, relaxes during crystallization accompanied by a shrinkage; a portion, γ_{e3}, relaxes thermally during the completion of crystallization (t_2) to mold parting (t_3); a portion, γ_{e4}, relaxes thermally after mold parting; and a portion, γ_{e5}, remains in the molded article as a frozen-in strain. Of these strains, the one which participates in the mold shrinkage is ($\gamma_{e2} + \gamma_{e3} + \gamma_{e4}$), and the one which participates in the annealing shrinkage and melting shrinkage is the frozen-in strain γ_{e5}. Consequently, it is assumed that, if the molding cycle is the same, the shrinkages become higher as the total strain γ_e becomes higher and the melt-relaxed strain γ_{e1} becomes lower. γ_{e1} becomes lower as the relaxation time λ becomes longer and the crystallization time t_c becomes shorter. After all, when shrinkage is viewed from molecular chain orientation, the rheological characteristics (γ_e, λ) and the crystallization characteristic (t_c) contribute to shrinkage. The shrinkage becomes higher as γ_e becomes higher, λ becomes longer, and t_c becomes shorter (Fig. 17).

According to the Rouse theory modified by Ferry,[1] the steady-state shear compliance J_e^0 is given by eq. (4):

$$J_e^0 = \frac{2}{5\rho RT} \cdot \frac{\overline{M}_z \cdot \overline{M}_{z+1}}{\overline{M}_w} \tag{4}$$

where ρ is the density of molten resin, R is the gas constant, T is the absolute temperature, and $\overline{M}_w$, $\overline{M}_z$, and $\overline{M}_{z+1}$ are the weight-, z-, and ($z + 1$)-average molecular weights, respectively. By use of eq. (4), the recoverable shear strain γ_e and its relaxation time λ are represented by eqs. (5) and (6), respectively:

$$\gamma_e = J_e^0 \tau = J_e^0 \eta \dot{\gamma} = \frac{2\eta}{5\rho RT} \cdot \frac{\overline{M}_z \cdot \overline{M}_{z+1}}{\overline{M}_w} \cdot \dot{\gamma} \tag{5}$$

$$\lambda = \frac{\eta}{G} = \frac{\tau/\dot{\gamma}}{\tau/\gamma_e} = \frac{\gamma_e}{\dot{\gamma}} = \frac{2\eta}{5\rho RT} \cdot \frac{\overline{M}_z \cdot \overline{M}_{z+1}}{\overline{M}_w} \tag{6}$$

where τ is the shear stress, $\dot{\gamma}$ is the shear rate, η is the shear viscosity, and G is the shear modulus. Although eq. (4) and hence eqs. (4) and (5) are strictly true
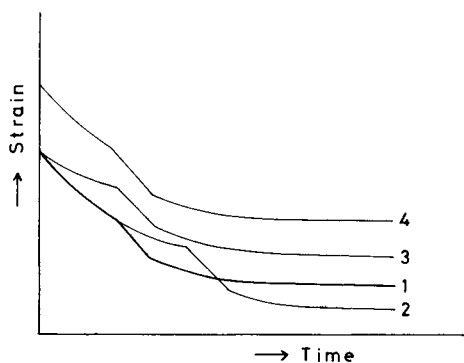

Fig. 17. Schematic diagram for variation in recoverable shear strains when γ_e, λ, and t_c change: (1) standard; (2) γ_e and λ are the same and t_c is longer; (3) γ_e and t_c are same and λ is longer; (4) t_c and λ are same and γ_e is higher.

in the low shear-rate range, they are not strictly true in the high shear-rate range as in the case of injection molding. However, γ_e and λ are relatively evaluated by eqs. (5) and (6), respectively, when the injection molding is carried out with different kinds of resins. Furthermore, since the mold and annealing shrinkages in the TD are independent of the kind of resin (Figs. 2 and 4), we assume that the crystallization characteristic (t_c) is the same. It is seen from eqs. (5) and (6) that, under the conditions of constant injection speed and cylinder temperature (accordingly, constant $\dot{\gamma}$ and T), γ_e and λ become higher as $\eta(\overline{M}_z\cdot\overline{M}_{z+1}/\overline{M}_w)$ becomes higher. η becomes higher as the molecular weight becomes higher (MFI becomes lower). $\overline{M}_z\cdot\overline{M}_{z+1}/\overline{M}_w$ becomes higher as the molecular weight becomes higher and the molecular weight distribution becomes broader. Consequently, γ_e and λ become higher as the molecular weight becomes higher (MFI becomes lower) and the molecular weight distribution becomes broader, and hence the shrinkages also become higher as the molecular weight increases (MFI becomes lower) and the molecular weight distribution becomes broader. The experimental results can thus be explained.

Next, we will discuss the relation between the recoverable shear strain and the thickness of the skin layer. Since PP melts crystallize under a high shear stress in injection molding, their molecular chains crystallize in an expanded state (orientation crystallization). At this time, not all expanded molecular chains orientation crystallize, but a portion become random coils due to their relaxation during the time before crystallization and cause crystallization (spherulization). The number of molecular chains that orientation crystallize (proportional to the thickness of the skin layer) must become larger as the degree of the expansion of the molecular chains becomes higher, their relaxation becomes slower, and the time before they crystallize becomes shorter. The degree of expansion of the molecular chains, the rate of the relaxation, and the time before crystallization are represented quantitatively by the recoverable shear strain γ_e, the relaxation time λ, and the crystallization time t_c. The thickness of the skin layer must become higher as γ_e becomes higher, λ becomes longer, and t_c becomes shorter. These circumstances are quite similar to those in the discussion on shrinkage described above, and it can be predicted easily that there is an intimate correlation between shrinkage and thickness of the skin layer, which manifests itself realistically in the form of linear relationships in the experimental results.

It can be said that shrinkage correlates closely with thickness of the skin layer through the recoverable shear strain which is governed by rheological and crystallization characteristics. These, in turn, are governed finally by the molecular structure of PP.

CONCLUSIONS

The effect of some molecular parameters on the mold shrinkage, annealing shrinkage, and melting shrinkage of injection-molded PP was studied. The mold shrinkage in the MD became higher as the MFI became lower and the molecular weight distribution became broader. Compared on the same MFI level, block copolymers with ethylene showed higher mold shrinkage in the MD than straight PPs. Random copolymers with ethylene and a low-tacticity PP showed lower mold shrinkage in the MD than the straight PPs. An FRPP showed very low mold shrinkage in the MD. Meanwhile, the mold shrinkage in the TD showed

a similar value (about 1.6%), regardless of the kind of resin, except for the FRPP, which showed a very low value.   The annealing shrinkage and melting shrinkage showed similar tendencies as the mold shrinkage.   The mold shrinkage and annealing shrinkage in the MD were in linear relationships with the thickness of skin layer having positive slopes.   The melting shrinkage in the MD was in a downward-curved relationship with the thickness of the skin layer having a positive slope, regardless of the cylinder temperature and the kind of resin. These facts suggest that variations in shrinkage with injection molding conditions (cylinder temperature) and with the kind of resin used were mainly due to the orientation effect of the molecular chains.

References

1. J. D. Ferry, *Viscoelastic Properties of Polymers*, Wiley, New York, 1960.
2. M. Fujiyama and S. Kimura, *Kobunshi Ronbunshu*, **32,** 581 (1975).
3. N. Takashima and K. Mizutani, *High Polym., Jpn.*, **12,** 504 (1963).
4. H. Keskkula and J. A. Shmitt, *J. Appl. Polym. Sci.,* **9,** 2666 (1965).
5. S. Onogi, T. Fujii, H. Kato, and S. Ogihara, *J. Phys. Chem.,* **68,** 1598 (1964).
6. W. W. Graessley, *J. Chem. Phys.,* **47,** 1942 (1967).
7. M. Fujiyama, H. Awaya, and S. Kimura, *J. Appl. Polym. Sci.,* **21,** 3291 (1977).
8. M. Fujiyama and S. Kimura, *Kobunshi Ronbunshu,* **32,** 591 (1975).
9. M. Fujiyama, *Kobunshi Ronbunshu,* **32,** 411 (1975).